

Accepted Manuscript

Dicoumarol derivatives: green synthesis and molecular modelling studies of their anti-LOX activity

Dušica Simijonović, Evangelia-Eirini Vlachou, Zorica D. Petrović, Dimitra J. Hadjipavlou-Litina, Konstantinos E. Litinas, Nevena Stanković, Nezrina Mihović, Milan P. Mladenović

PII: S0045-2068(18)30567-4
DOI: <https://doi.org/10.1016/j.bioorg.2018.07.021>
Reference: YBIOO 2440

To appear in: *Bioorganic Chemistry*

Received Date: 11 June 2018
Revised Date: 17 July 2018
Accepted Date: 18 July 2018

Please cite this article as: D. Simijonović, E-E. Vlachou, Z.D. Petrović, D.J. Hadjipavlou-Litina, #.E. Litinas, N. Stanković, N. Mihović, M.P. Mladenović, Dicoumarol derivatives: green synthesis and molecular modelling studies of their anti-LOX activity, *Bioorganic Chemistry* (2018), doi: <https://doi.org/10.1016/j.bioorg.2018.07.021>

This is a PDF file of an unedited manuscript that has been accepted for publication. As a service to our customers we are providing this early version of the manuscript. The manuscript will undergo copyediting, typesetting, and review of the resulting proof before it is published in its final form. Please note that during the production process errors may be discovered which could affect the content, and all legal disclaimers that apply to the journal pertain.



Dicoumarol derivatives: green synthesis and molecular modelling studies of their anti-LOX activity

Dušica Simijonović,^{*a} Evangelia-Eirini Vlachou,^b Zorica D. Petrović,^a Dimitra J. Hadjipavlou-Litina,^c Konstantinos E. Litinas,^b Nevena Stanković,^d Nezrina Mihović,^d Milan P. Mladenović^d

^a *University of Kragujevac, Faculty of Science, Department of Chemistry, Radoja Domanovića 12, 34000 Kragujevac, Serbia.*

^b *Laboratory of Organic Chemistry, Department of Chemistry, Aristotle University of Thessaloniki, Thessaloniki 54124, Greece.*

^c *Department of Pharmaceutical Chemistry, School of Pharmacy, Faculty of Health Sciences, Aristotle University of Thessaloniki, Thessaloniki 54124, Greece.*

^d *Kragujevac Center for Computational Biochemistry, Faculty of Science, University of Kragujevac, Radoja Domanovića 12, 34000 Kragujevac, P.O. Box 60, Serbia*

Abstract

Dicoumarol derivatives were synthesized in the InCl_3 catalyzed pseudo three-component reactions of 4-hydroxycoumarin with aromatic aldehydes in excellent yields. The reactions were performed in water under microwave irradiation. All synthesized compounds were characterized using NMR, IR, and UV-Vis spectroscopy, as well as with TD-DFT. Obtained dicoumarols were subjected to evaluation of their *in vitro* lipid peroxidation and soybean lipoxygenase inhibition activities. It was shown that five of ten examined compounds (**3e**, **3h**, **3b**, **3d**, **3f**) possess significant potential of antilipid peroxidation (84 to 97%), and that compounds **3b**, **3e**, **3h** provided the highest soybean lipoxygenase (LOX-Ib) inhibition ($\text{IC}_{50} = 52.5 \mu\text{M}$) and **3i** somewhat lower activity ($\text{IC}_{50} = 55.5 \mu\text{M}$). The bioactive conformations of the best LOX-Ib inhibitors were obtained by means of molecular docking and molecular dynamics. It was shown that, within the bioactive conformations interior to LOX-Ib active site, the most active compounds form the pyramidal structure made of two 4-hydroxycoumarin cores and a central phenyl substituent. This form serves as a spatial barrier which prevents LOX-Ib $\text{Fe}^{2+}/\text{Fe}^{3+}$ ion activity to generate the coordinative bond with the C13 hydroxyl group of the α -linoleate. It is worth pointing out that the most active compounds **3b**, **3e**, **3h** and **3i** can be candidates for further examination of their *in vitro* and *in vivo* anti-inflammatory activity and that molecular modeling study results provide possibility to screen bioactive conformations and elucidate the mechanism of dicoumarols anti-LOX activity.

Keywords: Dicoumarol derivatives, InCl_3 catalyzed synthesis, microwave irradiation, anti-inflammatory activity, molecular docking, molecular dynamics

Corresponding author:

*D. Simijonović: tel.: +381-34-336-223; +381-34-335-039; e-mail: dusicachem@kg.ac.rs

1. Introduction

It is known that coumarin derivatives exhibit a lot of pharmacological and biological activities [1]. 4-Hydroxycoumarin, between them, represent significant structural fragment for many synthetic and natural products [2]. Therefore, they are important precursors in organic synthesis and useful pharmacophores in medicinal chemistry. Their derivatives, exert broad spectrum of biological activities such as anticoagulant [3], antibacterial [4,5], antifungal [5], antiviral [6], antitumor [7], antioxidant [8,9] and anti-inflammatory [10]. Warfarin (**I**) (Fig. 1) is an anticoagulant drug in extended clinical use [11,12]. Derivatives of **I** [10] as well as the natural product dicoumarol [13,14] (**II**) and the synthetic phenprocoumon [11,12] (**III**) are also anticoagulants. Moreover, the above compounds present other biological activities such as anticancer [2a,15], HIV-1 integrase inhibition [16], and urease inhibition [17].

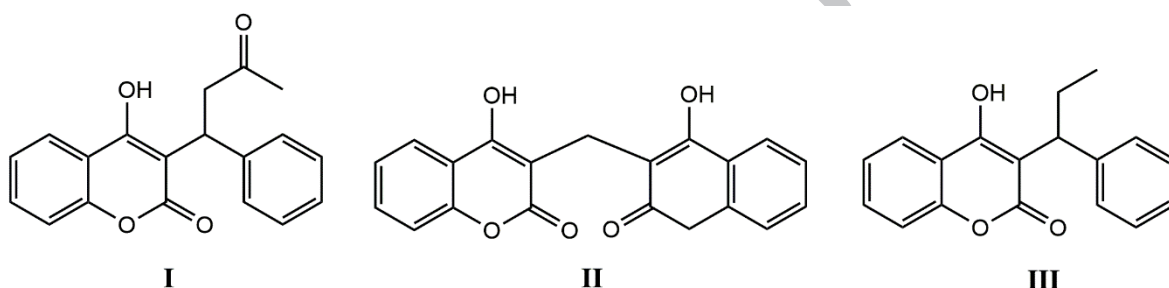


Fig. 1. Some natural and synthetic coumarin derivatives used as anticoagulant drugs

Dicoumarol derivatives are generally synthesized through the reaction of 4-hydroxycoumarin and aldehydes using different catalysts and media. Recently, several methods have been reported for the synthesis of these compounds, which includes the use of different catalyst systems such as p-dodecylbenzenesulfonic acid/piperidine [18], molecular iodine [19], ionic liquids with Lewis acid and/or Bronsted acid sites [20], SO₃H functionalized ionic liquids [21], Zn(proline)₂ [22], heteropoly acid [23], sodium dodecyl sulfate [24], sulfated titania [25], nano silica catalysts [26], propane-1,2,3-triyltris (hydrogen sulfate) [27], Ce₂(SO₄)×4H₂O [28], Fe₃O₄ nanoparticles [29], reflux in alcohols [30,31] or heating in aqueous NaCl solution [32]. However, although in the literature there are a lot of studies relating to the synthesis of dicoumarols under classical conditions, only a few articles can be found related to the synthesis of these compounds under microwave assisted conditions [33,35]. Microwaves are essential for the application of green chemistry in science and technology [36]. Water is a characteristic green solvent, as it is readily available with non-toxicity, non-flammability and high heat capacity.

The lipoxygenases (LOXs) are enzymes which can be found in animals, plants, and fungi. These enzymes catalyze the oxidative metabolism of polyunsaturated fatty acids. Linoleic acid is the primary substrate in the reaction of oxygenation of polyunsaturated fatty acids catalyzed by plant LOX, while the mammalian isozymes mainly catalyze the metabolism of arachidonic acid [37]. The leukotrienes are products of this metabolism. Leukotrienes, lipid mediators and

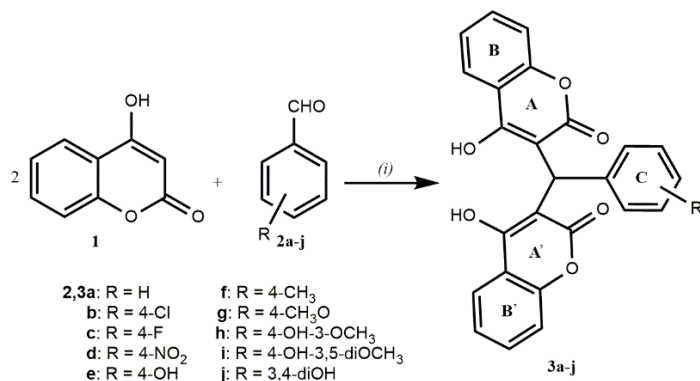
bioregulators, have been associated with various pathological processes, such as bronchial asthma, inflammation, and cancer and that they can regulate tumor progression, apoptosis, and migration through a lot of signaling [38]. In the literature are described a few types of lipoxygenases inhibitors: *i*) redox-active compounds *ii*) iron-ligand inhibitors with weak redox-active properties, and *iii*) non-redox-type inhibitors [39]. Among many investigated compounds, coumarin derivatives, belong to the group of redox-active lipoxygenase inhibitors. Although, the mechanism of action of the available LOX inhibitors is not yet fully elucidated, they could significantly contribute to the suppressing of the negative LOX impact on human health [40]. Hence, the finding of effective LOX inhibitors is challenge for numerous scientific laboratories.

In the course of our interest in the synthesis of coumarin derivatives under MW irradiation [41], we wish to report here the application of InCl_3 catalysis in water, as green solvent, under MW irradiation for the synthesis of these compounds. To our best knowledge, InCl_3 has been used only for the reactions of dimedone and aldehydes under heating [42], leading to the synthesis of fused pyran derivatives. In addition, obtained dicoumarol derivatives were characterized using NMR, IR, and UV-Vis spectroscopy and were tested as inhibitors of lipid peroxidation and soybean lipoxygenase (LOX-Ib). Since docking study provide possibility to screen the binding affinity and orientation of bioactive compounds at the active site of the enzyme, molecular docking and molecular dynamics studies of the most potent LOX-Ib inhibitors were performed.

2. Results and discussion

2.1. Chemistry

The studied reactions and obtained products are depicted in Scheme 1. The reaction was performed by treatment of 4-hydroxycoumarin (**1**) with benzaldehyde (**2a**) in the presence of 10 mol% InCl_3 in water, under MW irradiation and by heating. After cooling and filtration of the reaction mixture, 3,3'-(phenylmethylene)bis(4-hydroxy-2H-chromene-2-one) (**3a**) was obtained [14,19] (90% yield) (Table 1, entry 1). In fact, this reaction is a pseudo three-component reaction by using twofold equivalents of 4-hydroxycoumarin (**1**) to benzaldehyde (**2**).



Scheme 1. Reaction of formation dicoumarol derivatives. Reagents and conditions: (i) **1** (1 mmol), **2** (0.5 mmol), H₂O, InCl₃ (0.05mmol), MW, 110°C.

Table 1. Synthesis of dicoumarols **3a-j**.

Entry	R	Product	Time (min)	Yield (%)
1	H	3a	20	90
2	4-Cl	3b	15	91
3	4-F	3c	15	93
4	4-NO ₂	3d	15	96
5	4-OH	3e	20	90
6	4-CH ₃	3f	20	85
7	4-CH ₃ O	3g	20	87
8	4-OH, 3-OCH ₃	3h	20	89
9	4-OH, 3,5-di-OCH ₃	3i	20	86
10	3,4-di-OH	3j	20	85

The analogous reactions with aldehydes **2b-j** led to the substituted dicoumarol derivatives **3a-j** in excellent yields (85-96%) (Table 1). Aldehydes with electron withdrawing group reacted faster (15 min.) producing the dicoumarols in a little better yield (Table 1, entries 2-4). Aldehydes with electron donating groups gave slightly lower yields and required longer reaction time (Table 1, entries 5-10).

2.2. Structural characterization

Synthesized dicoumarols (**3a-3j**) were experimentally characterized by ¹H and ¹³C NMR, IR and UV-Vis spectroscopy, as well as with melting points. In addition, the structures of these compounds were elucidated based on UV-Vis simulated spectral properties. It is worth pointing out that UV-Vis spectral characterisation of these compounds is reported here for the first time.

In the ¹H NMR spectra of all compounds singlets originating from protons of benzylic carbon, linkage for two 4-hydroxycoumarin moieties and for aromatic ring **C** appear in the range of 6.01-6.12 ppm. The aromatic protons of rings **B**, **B'** and **C** were observed in region of 6.42-8.19 ppm. Hydroxy groups of 4-hydroxycoumarin part of molecule appear around 11.30 and 11.50 ppm as broad singlets. In the spectra of compounds **3f-3i**, singlets originating from protons of methyl group (**3f**) and methoxy groups (**3g-3i**) bonded for aromatic ring at 2.34, 3.79 and 3.75 ppm were observed. In ¹³C NMR spectra of all dicoumarol derivatives, benzylic carbon atom appears around 36 ppm. In the range of 104-147 ppm, peaks are assigned to aromatic carbon atoms. Peaks observed at around 152, 166, and 169 ppm were assigned to C-O, C-OH and C=O carbon atoms. The spectra of compounds **3f-3i**, contain additional peaks at around 21 and 56 ppm for methyl and methoxy group, respectively. The IR spectra of the all compounds contain weak bands at about 3400, 3060, and 1350 cm⁻¹, which correspond to the vibration of O-H and C-OH groups. The peaks in region 1615-1670 cm⁻¹ are assigned to the C=O of lactone ring,

while bands present at about 1560 and 1600 cm^{-1} originate from stretching vibration of double bond and aromatic rings.

In the UV-Vis spectra of all compounds (experimental and simulated) three major absorption bands appear around 230 nm, 280 and 310 nm, Figs. 2 and S1. It is worth pointing out, that in all simulated spectra bands over 300 nm are somewhat redshifted.

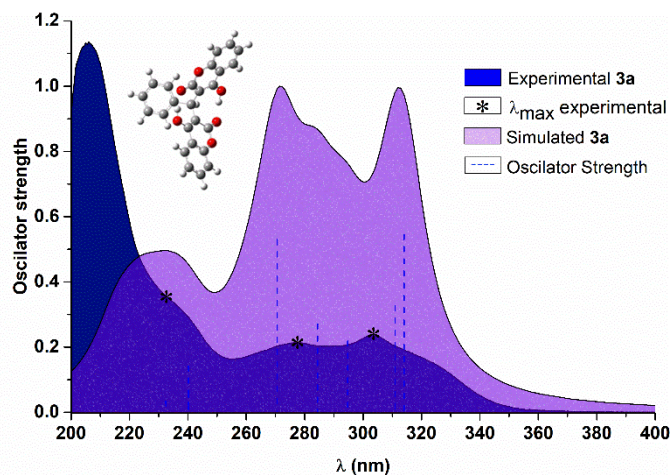
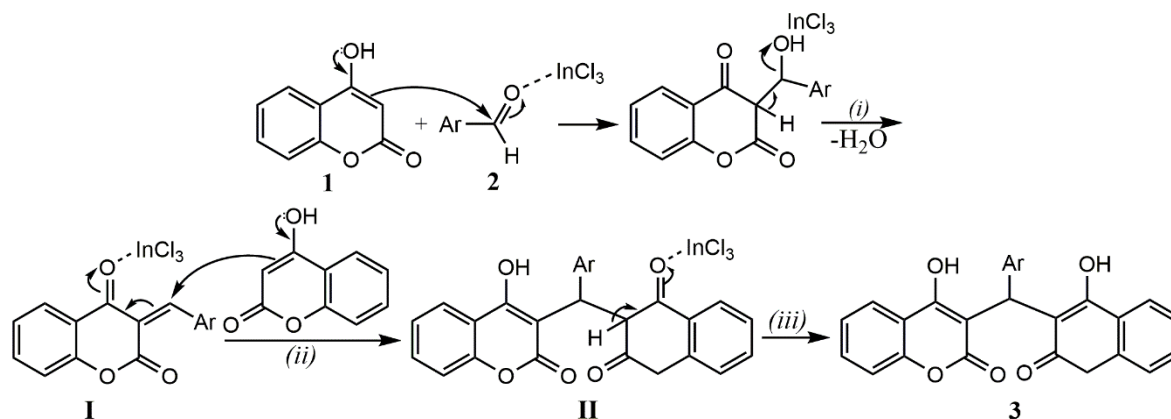


Fig. 2. Experimental and simulated UV-Vis spectra of compound **3a**

To distinguish the parts of molecules responsible for electronic transitions, Kohn–Sham orbitals were constructed, Fig. S2-11. Inspection of UV-Vis spectra and constructed orbitals revealed that bands at lower wavelength (about 230 nm in experimental spectra) are appearing owing to relatively large energy, but relatively small spatial separation, while the higher wavelengths are consequence of relatively smaller energy separation of corresponding HOMO and LUMO, as well as small spatial separation (HOMO, LUMO, and LUMO+1 share same regions, Fig. S2-11). Detailed UV-Vis characterization is provided in Supplementary material.

A possible mechanistic pathway for the formation of obtained dicoumarols is given in Scheme 2. 4-Hydroxycoumarin (**1**) is firstly reacted with an aromatic aldehyde in the presence of InCl_3 , as a Lewis acid which increase electrophilicity of carbonyl. After the liberation of water, intermediate **I** was formed. The electron-withdrawing groups in aromatic ring of aldehydes facilitate the addition. This is a Knoevenagel type reaction. Next, second molecule of **1** attacks the α,β -unsaturated ketone **I**, *via* a Michael addition, to generate the intermediate **II**. Enolization of the latter intermediate resulted to substituted dicoumarols **3**.



Scheme 2. The reaction pathway toward the formation of dicoumarols; (i) Knoevenagel type reaction; (ii) Michael-addition; (iii) enolization.

Preliminary biological tests, which was done by using the AAPH assay [41a,b], revealed that the examined compounds **3e**, **3h**, **3b**, **3d**, **3f** presented the high activity, ranged from 84 to 97%, whereas **3j**, **3a**, **3i**, **3g**, **3c** showed moderate (39-71%) inhibition of lipid peroxidation, Fig. 3.

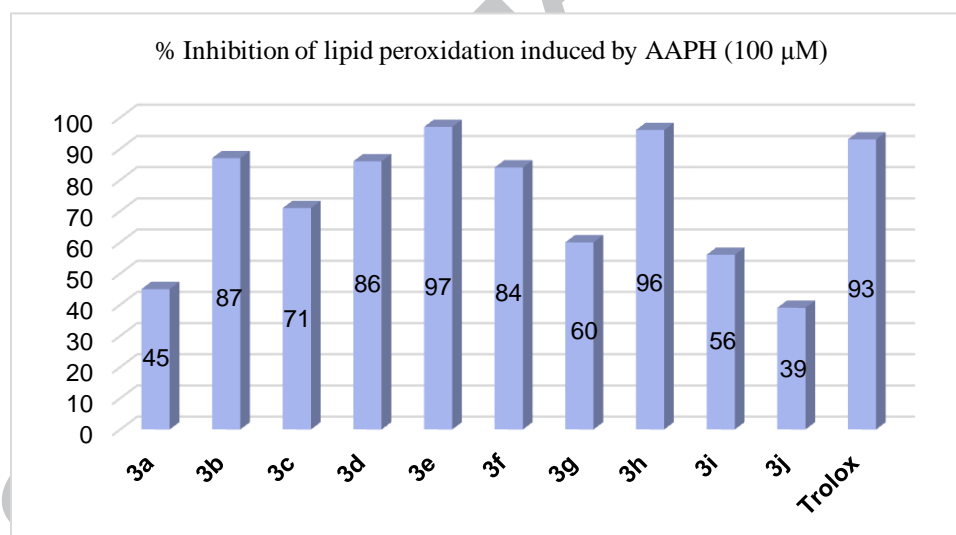


Fig. 3. *In vitro* inhibition of lipid peroxidation (LP%) at 100 μ M for compounds **3a-3j** and reference compound (Trolox).

Data for the scavenging DPPH radical activity of compounds **3i**, **3j** can be found in the literature [9], but not for dicoumarols anti-LOX activity. Since lipoxygenation occurs *via* a carbon centered radical, it is to be expected that compounds with potent anti-lipid peroxidation will exert good LOX inhibition, also. Therefore, all compounds were tested as inhibitors of soybean lipoxygenase [41a,b], an enzyme implicated in arachidonic acid cascade and different pathological disorders. The compounds **3b**, **3e**, **3h** provided the highest LOX inhibition (IC_{50} =

52.5 μM), followed by activity of **3i** ($\text{IC}_{50} = 55.5 \mu\text{M}$) and **3d** ($\text{IC}_{50} = 60 \mu\text{M}$). Compounds **3c**, **3f** and **3a** exhibit activity in range of 76-92 μM , while compounds **3j** and **3g** exert the less activity (39% and 43% at 100 μM), Table 2.

Table 2. *In vitro* LOX inhibition (IC_{50})/% at 100 μM for compounds **3a-3j** and reference compound (NDGA).

Compounds	IC_{50} (μM) or % at 100 μM
3a	92 μM
3b	52.5 μM
3c	76 μM
3d	60 μM
3e	52.5 μM
3f	76 μM
3g	43%
3h	52.5 μM
3i	55.5 μM
3j	39%
NDGA	5.5 μM

2.3. Molecular modeling study

2.3.1. Bioactive conformations of compounds **3b**, **3e**, **3h**, and **3i** during the LOX-Ib inhibition

The lack of the literature data regarding to molecular docking study of coumarin derivatives as lipoxygenase inhibitors [39a,b] was motivated us to examine the binding affinity of synthesized dicoumarols and their orientation at the active site of the enzyme. Bioactive conformations of the best active LOX-Ib dicoumarol inhibitors were revealed by means of flexible ligand-rigid enzyme (molecular docking, Fig. 4) and induced fit (Molecular Dynamics, MD, Figs. 5-8) simulations. Both structure-based methodologies supported each other by virtue of accomplished results, thus confirming that the obtained best docked/fitted conformations are bioactive ones. Within the enclosed series, the highest potency during the soybean lipoxygenase inhibition was exerted by four compounds, namely **3b** (Fig. 4A), **3e** (Fig. 4B), **3h** (Fig. 4C), and **3i** (Fig. 4D), respectively. Thus, within the bioactive conformation of **3b**, two 4-hydroxycoumarin cores and *p*-chlorobenzene are joined into the pyramidal structure, with the chlorine atom, as a top of the pyramid, positioned inside the hydrophobic pocket compiled of Thr255, Leu534, Leu537, Leu542, and Leu750. The obtained conformation is snugly situated indoors the active site: the **3b**-LOX-Ib reached its stability after 0.6 ns of induced fit simulations and remained stable onwards (Fig. 5A). The *p*-chlorobenzene scaffold of **3b** is involved in electrostatic interactions with the side chain hydroxyl group of Thr255 or imidazole ring of His500; particular interactions are interchanging during the 90% of Molecular Dynamics (MD) run time (1.2 ns) (Figs. 5C, 9A). Moreover, the benzene moiety is for 30% of MD time involved in π - π hydrophobic interactions with His500, whereas for the remaining time the scaffold is facing the rest of the LOX-Ib active site hydrophobic pocket (Figs. 5C, 9A). Being positioned, the *p*-chlorobenzene scaffold seems to

prevent the LOX-Ib activity to catalyze its own reaction, *i.e.* the oxygenation of linoleic acid: the *p*-chlorobenzene scaffold appears to be the spatial barrier for LOX-Ib Fe²⁺/Fe³⁺ ion, where the HO-Fe³⁺ cofactor form facilitates the C13 hydroperoxidation of α -linoleate towards 9Z,11E,13S,15Z-13-hydroperoxyoctadeca-9,11,15-trienoate [43]. This can be considered as a key factor for soybean lipoxygenase inhibition and anti-inflammatory activity of the most active compounds. In each of the scenarios, the generation of the pyramidal structure is a consequence of 4-hydroxycoumarin cores interactions. Hence, within the best docked bioactive conformation of **3b**, either the lactone carbonyl oxygen of the first coumarin core or the hydroxyl group at C4 of the second coumarin core establish electrostatic interactions with His495 (Figs. 5C, 9A), a residue that is involved in the generation of Fe²⁺/Fe³⁺ octahedral complex within the enzyme's active site. The phenyl part of the first 4-hydroxycoumarin core also establishes weak hydrophobic interactions with Thr552 and strong steric clash with Trp496 (Figs. 5C, 9A). On the other hand, the hydroxyl group at C4 of the second 4-hydroxycoumarin core is narrow to a strong hydrogen bond with the side chain amide carbonyl of Gln419 ($d_{\text{HB}} = 2.782 \text{ \AA}$) (Figs. 5C, 9A). The orientation of the first 4-hydroxycoumarin stays conserved during time, whereas the second coumarin core is slightly rotated in a manner that the lactone carbonyl oxygen and the oxygen from the pyrone part of the 4-hydroxycoumarin core are potent hydrogen bond acceptors to either Gln491 ($d_{\text{HB}} = 2.696 - 2.804 \text{ \AA}$, 83% of MD time) or Gln693 ($d_{\text{HB}} = 2.904 - 3.206 \text{ \AA}$, 10% of MD time) (Figs. 5C, 9A). Particular hydrogen bonds formation is facilitated by the hydrophobic clash between the phenyl part of the second 4-hydroxycoumarin core His500 (weak attraction) and Phe553 (strong and stable confrontation, 85% of MD time) (Figs. 5C, 9A).

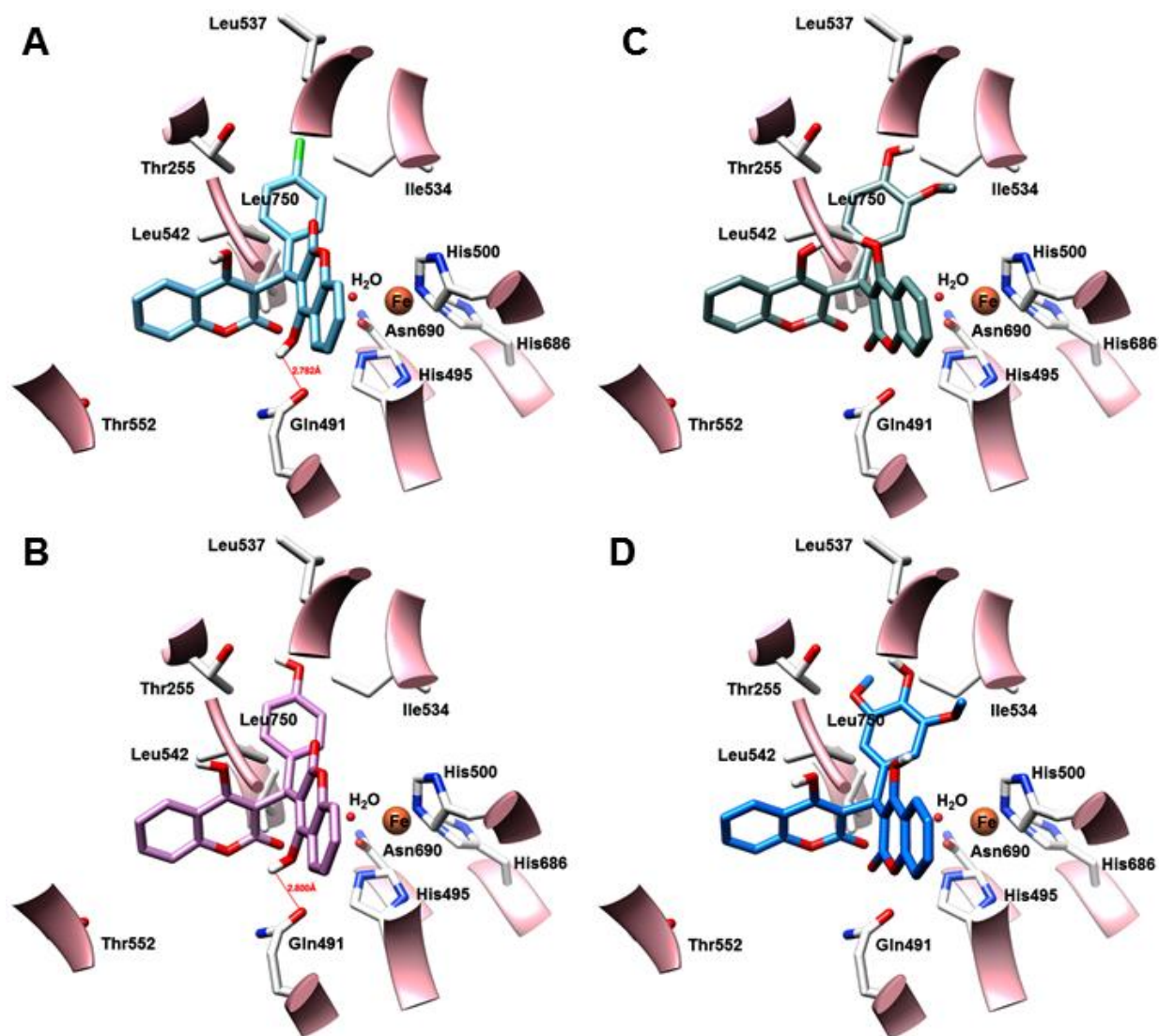


Fig. 4. The bioactive conformation of **3b** (A); **3e** (B); **3h** (C); **3i** (D). The LOX-Ib amino acids are presented in white, the LOX-Ib ribbon is colored in pink. For the clarity purpose, only polar hydrogen atoms are presented.

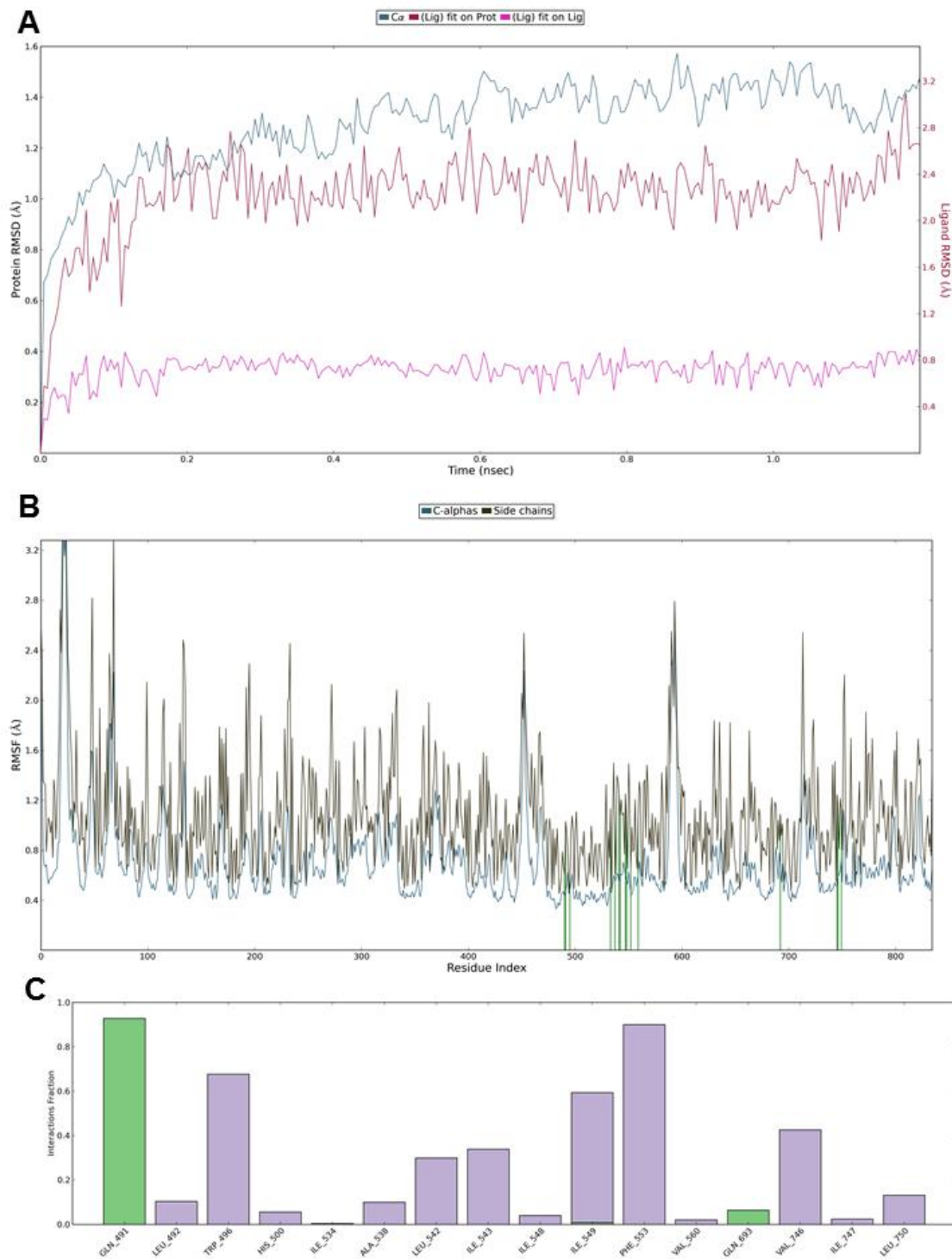


Fig. 5. RMSDs (A), RMSFs (B) and Interaction diagrams (C) of **3b** in complex with LOX-Ib. Green bars present hydrogen bonds, purple bars hydrophobic interactions, pink bars ionic interaction, blue bars water bridges

Further on, compound **3e** (Figs. 4B, 6A) is of comparable activity and conformation with **3b**, with the difference that *p*-hydroxybenzene is engaged *via* hydroxyl group in electrostatic interactions with Thr255 and in hydrophobic and/or induced dipole interactions with the hydrophobic pocket. Particular electrostatic interaction turns during the induced fit alignment into the strong and stable hydrogen bond between the hydroxyl group of the *p*-hydroxybenzene moiety and Thr255 ($d_{\text{HB}} = 2.793 - 2.912 \text{ \AA}$, 53% of MD time) (Figs. 6C, 9B). In addition, while the hydroxyl group of the *p*-hydroxybenzene scaffold is a hydrogen bond donor to the **3e**-Ile835-H₂O-Fe hydrogen bond-water bridge network ($d_{\text{HB}} = 4.125 - 5.563 \text{ \AA}$, 26% of MD time) between the anti-inflammatory agent and LOX-Ib iron ion (Figs. 6C, 9B). On this way, **3e** is indirectly associated with Fe ion, interrupting its ability to generate the coordinative bond with the hydroperoxide derivative of linoleic acid (13-HPOD) as LOX-Ib natural substrate. On the other hand, the lactone carbonyl of the first 4-hydroxycoumarin core of **3e** is bound to hydrogen bonds with either Gln693 ($d_{\text{HB}} = 2.517 - 2.716 \text{ \AA}$, 73% of MD time) or Gln491 ($d_{\text{HB}} = 2.314 - 2.552 \text{ \AA}$, 78% of MD time) (Figs. 6C, 9B). In addition, particular hydrogen bond network is completed by the contribution of the hydroxyl group at C4 of the second 4-hydroxycoumarin core which throughout the entire period of simulation stays in the strong hydrogen bond with the side chain amide carbonyl of Gln419 ($d_{\text{HB}} = 2.693 - 2.954 \text{ \AA}$, 83% of MD time) (Figs. 5C, 8B). Alike of **3b**, there is no rotation of the second 4-hydroxycoumarin core. Established hydrogen bond network most certainly contributes to high activity of **3b**. Another valuable interconnection is the hydrogen bond between the lactone carbonyl of the second 4-hydroxycoumarin core and His500 ($d_{\text{HB}} = 2.216 - 2.454 \text{ \AA}$, 83% of MD time) (Figs. 5C, 8B), an amino acid that is coordinatively bonded to Fe ion. This the second level of **3e**'s indirect association with Fe ion.

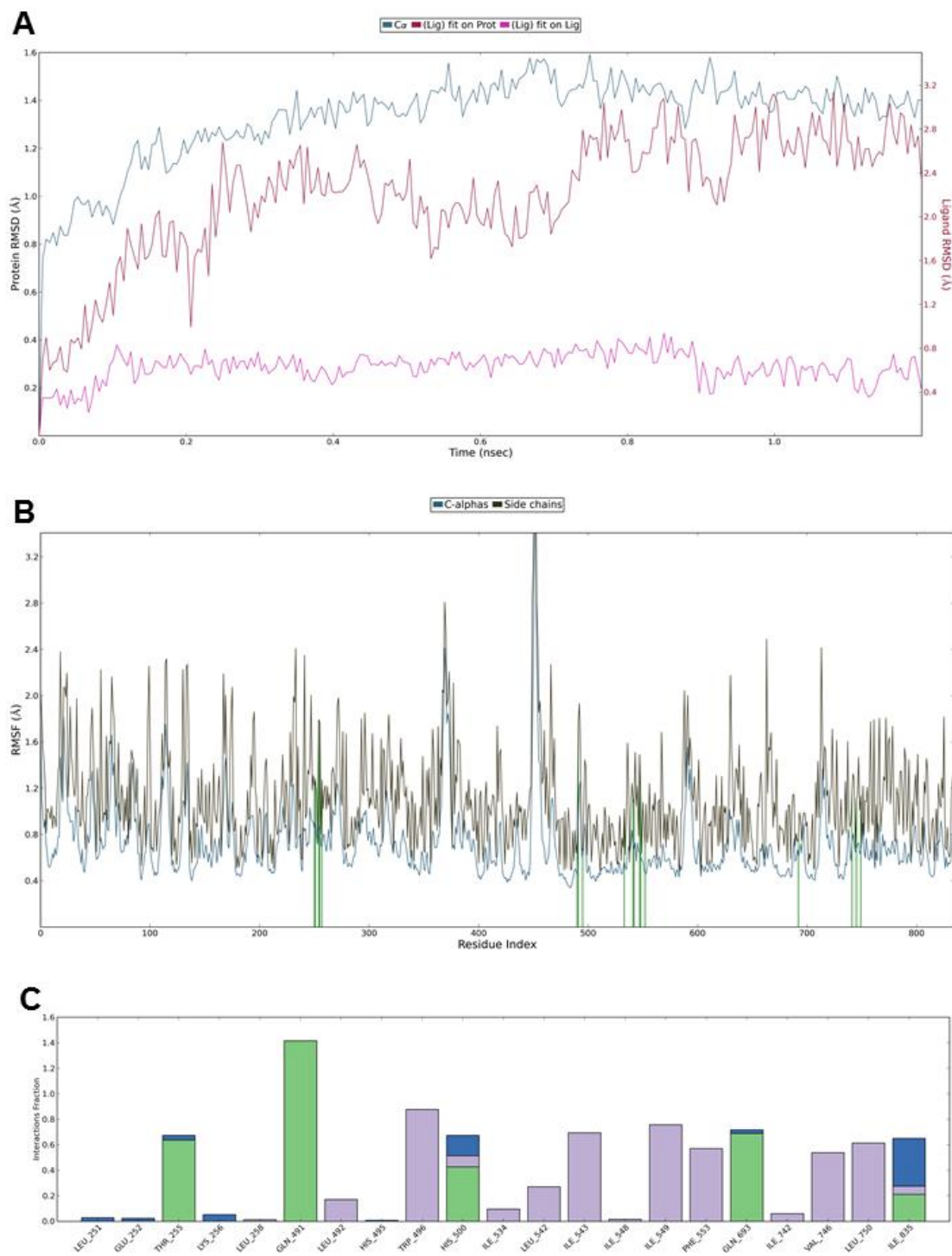


Fig. 6. RMSDs (A), RMSFs (B) and Interaction diagrams (C) of **3e** in complex with LOX-Ib. Green bars present hydrogen bonds, purple bars hydrophobic interactions, pink bars ionic interaction, blue bars water bridges

The introduction of the additional *m*-OCH₃ group causes the comparable activity but slightly different alignment of compound **3h** (Figs. 4C, 7A). The compound is, due to the contribution of *m*-OCH₃ moiety, still comfortably situated into the hydrophobic chamber. Thus, the newly introduced *m*-OCH₃ group is facing the pocket where the metal ion is stored, whereas the *p*-OH group is turning from electrostatic site to a hydrogen bond acceptor for Thr255. The established hydrogen bond, or its Thr255-H₂O-**3h** variation, remains stable through time until reaching the 0.6 ns of MD time. The similar observation is for the contemporaneously formed **3h**-Ile835-H₂O-Fe hydrogen bond-water bridge network ($d_{\text{HB}} = 4.125 - 5.563 \text{ \AA}$, 26% of MD time) (Figs. 7C, 9C). By being involved in the precise dispersed double hydrogen bond network, **3h** exerts high level of anti-inflammatory activity. However, after the 0.6th ns of simulation time, only the hydrogen bonds with Gln693 ($d_{\text{HB}} = 2.491 - 2.638 \text{ \AA}$, 62% of MD time) or Gln491 ($d_{\text{HB}} = 2.443 - 2.784 \text{ \AA}$, 55% of MD time) are formed (Figs. 7C, 9C), as previously described for **3b** and **3e**, thus maintaining the activity of **3h** on remarkable level. Required hydrogen bonds are not formed in the best docked conformation, only upon the induced fitting.

Similar conformation to **3h** is adopted by **3i** (Figs. 4D, 8A), mainly due to the existence of *m,m'*-dimethoxy-*p*-hydroxybenzene. The *m*-methoxy scaffold generates hydrophobic interactions *via* methyl group with Leu537, whereas the methyl group of the *m'*-methoxy moiety is in steric hindrance with Ile534. There are no hydrogen bonds with Thr255 or Ile835-H₂O-Fe network (Figs. 8C, 9D). The *m'*-methoxy moiety oxygen is electrostatically attracted by His500, another coordinative bond donor for iron. Besides the expressive hydrophobic influence of *m,m'*-dimethoxy-*p*-hydroxybenzene, compound **3i** owns its high anti-inflammatory potential to already well accredited hydrogen bonds with Gln693 ($d_{\text{HB}} = 2.372 - 2.783 \text{ \AA}$, 84% of MD time) or Gln491 ($d_{\text{HB}} = 2.673 - 2.841 \text{ \AA}$, 61% of MD time) (Figs. 8C, 9D). Summarized induced fit interactions for compounds **3b**, **3e**, **3h**, and **3i** are depicted by Fig. 9. The discussion of bioactive conformation-activity correlation of the remaining less active compounds is reported as Supplementary material (**Bioactive conformations of compounds 3d, 3f, 3c, 3a, 3g and 3j during the Lox-Ib inhibition** section, Fig. S12).

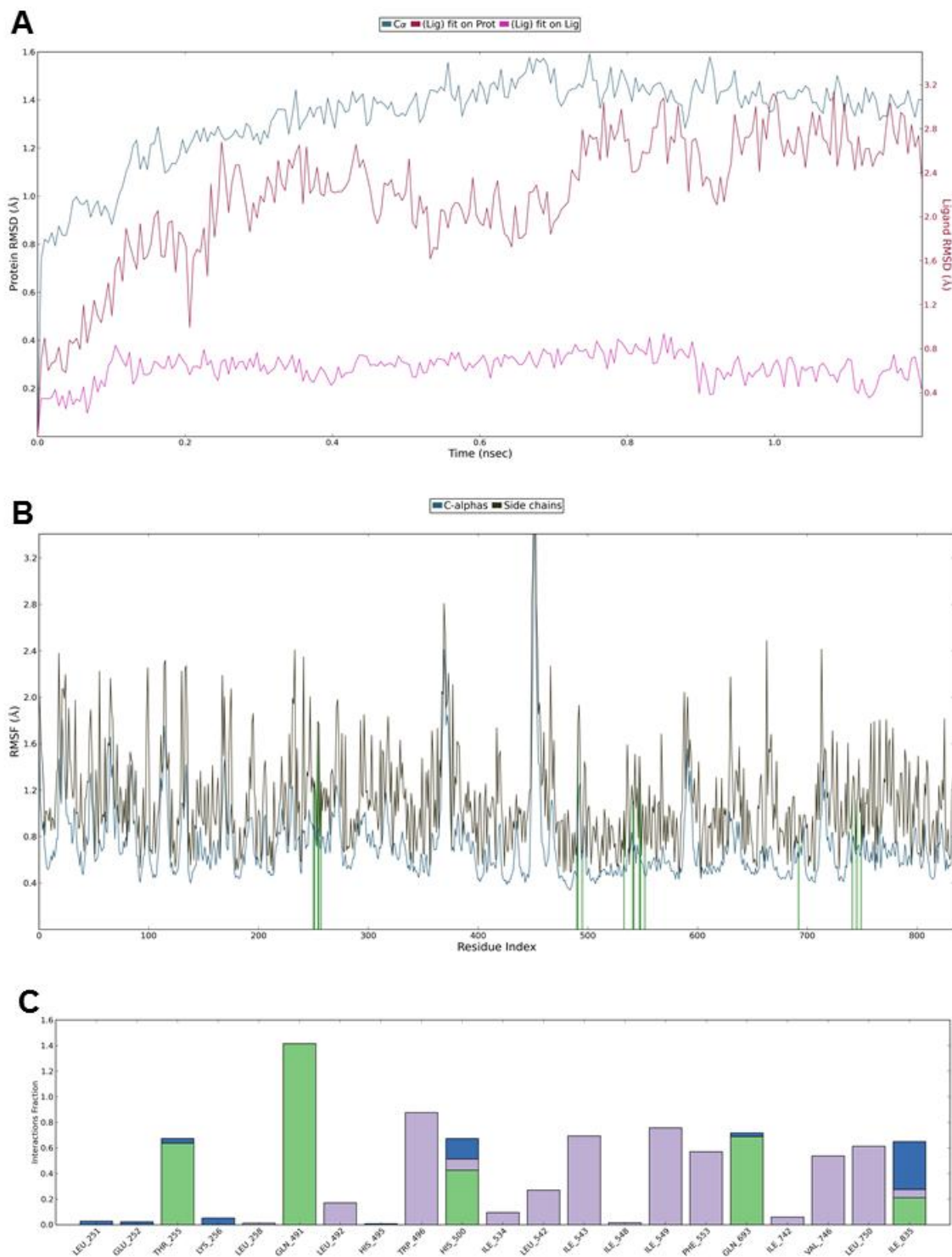


Fig. 7. RMSDs (A), RMSFs (B) and Interaction diagrams (C) of **3h** in complex with LOX-Ib. Green bars present hydrogen bonds, purple bars hydrophobic interactions, pink bars ionic interaction, blue bars water bridges

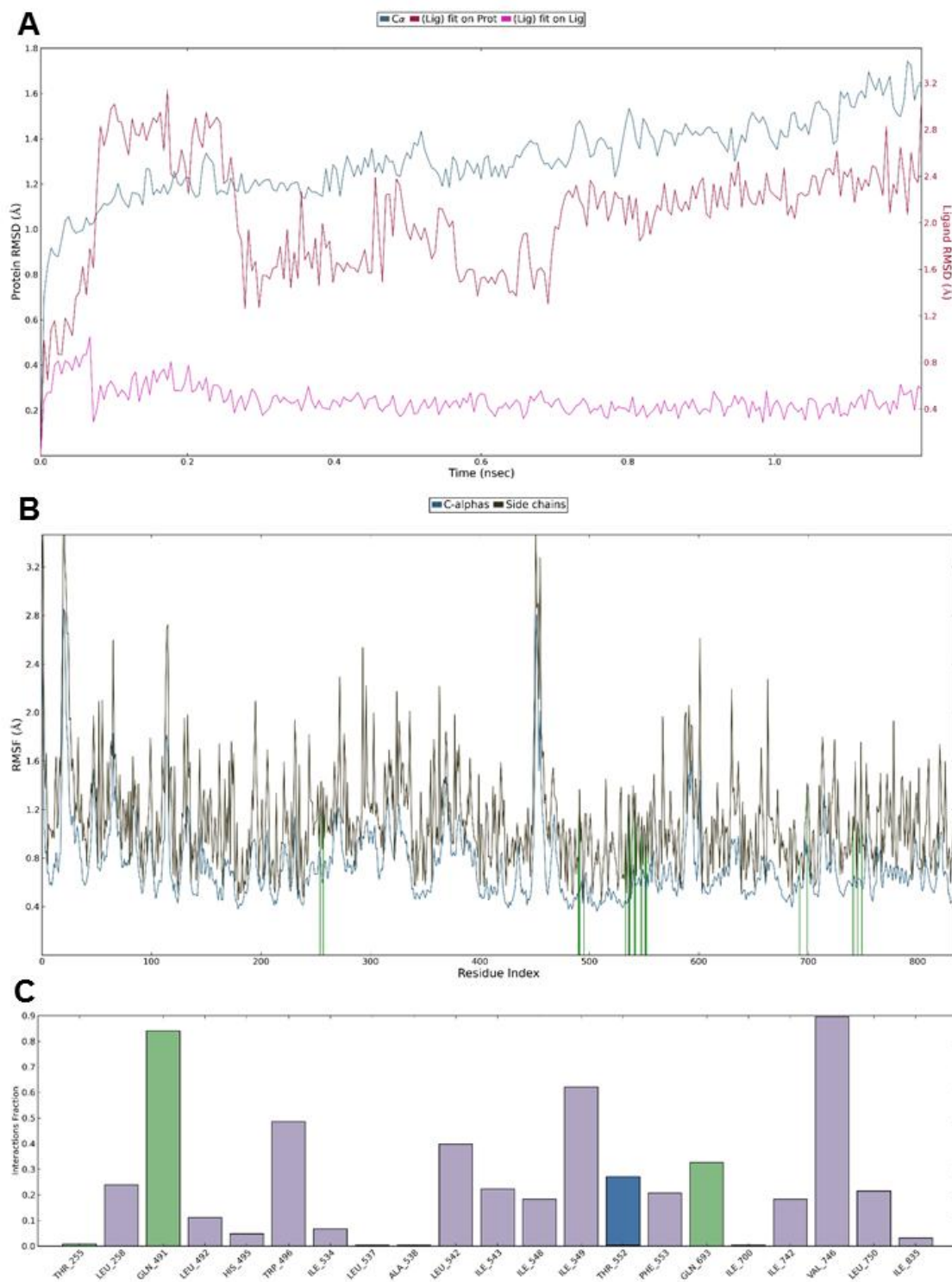


Fig. 8. RMSDs (A), RMSFs (B) and Interaction diagrams (C) of **3i** in complex with LOX-Ib. Green bars present hydrogen bonds, purple bars hydrophobic interactions, pink bars ionic interaction, blue bars water bridges

best LOX-Ib dicoumarol inhibitors were obtained by means of molecular modeling study. Structural insights based on molecular docking revealed that the most active compounds form the compact pyramidal structure made of two 4-hydroxycoumarin cores and a central phenyl substituent. This pyramidal structure is key reason for the formation strong hydrogen bonds and hydrophobic interactions with the important amino acid side chains in enzyme active site. This compact skeleton serves as a spatial barrier which is capable to prevent the C13 hydroperoxidation of enzyme substrate and its pro-inflammatory role. On the basis of the obtained results one can conclude that compounds **3b**, **3e**, **3h** and **3i** can be candidates for the further examination of their *in vitro* and *in vivo* anti-inflammatory activity and that may be useful for the elucidation of the mechanism of the anti-LOX-Ib dicoumarols activity.

4. Experimental

4.1. Material and methods

Melting points were determined on a Kofler hot-stage apparatus and are uncorrected. IR spectra were obtained with a Perkin-Elmer 1310 spectrophotometer as KBr pellets. The UV-Vis spectra were measured at room temperature within the 200-500 nm range on the Agilent Technologies, Cary 300 Series UV-Vis Spectrophotometer. A solution of 2.5×10^{-5} M of each compound was prepared in methanol and then 2 mL of the corresponding solution was injected into the 10 mm quartz cell and recorded spectrum. NMR spectra were recorded on an Agilent (Varian) 500/54 (500 MHz and 125 MHz) for ^1H and ^{13}C , respectively using CDCl_3 and DMSO as solvent and TMS as an internal standard. *J* values are reported in Hz. Mass spectra were determined on a LCMS-2010 EV Instrument (Shimadzu) under Electrospray Ionization (ESI) conditions. The MW experiments were performed in a Biotage (Initiator 2.0) scientific MW oven.

4.2. General procedure

The synthesis of dicoumarol derivatives under InCl_3 catalysis. In a 5 ml vessel, for reactions in MW oven, 4-hydroxycoumarin (**1**) (0.162 g, 1 mmol) and benzaldehyde (**2a**) (53 mg, 0.5 mmol) were added in H_2O (2 ml) followed by InCl_3 (11mg, 0.05 mmol). The mixture was irradiated at 110°C for 20 min. After cooling, the precipitate was filtered, washed thoroughly with H_2O (5×2 ml) and dried under vacuum to give **3a** (0.185 g, 90% yield). All dicoumarol derivatives **3a-3j** were characterized with melting point, ^1H NMR, ^{13}C NMR, IR and UV-Vis spectra, while compound **3a** was characterized additionally with MS (ESI) spectra. The characterizations of compound **3a** is given in main part of the manuscript, while for compounds **3b-3j** in Supplementary material, as well as copies of ^1H NMR, ^{13}C NMR and UV-Vis spectra for all compounds. It is worth pointing out that analytical and spectral data for obtained compounds are in accordance with literature data [6b,9,19,26b,32].

3,3'-(Phenylmethylene)bis(4-hydroxy-2H-chromene-2-one) (**3a**) [14,19,32]: (90% yield) white solid, m.p. $228-230^\circ\text{C}$ (EtOH-DCM), IR (KBr): 3443, 3068, 2927, 1660, 1604, 1617, 1568, 1496, 1149, 1347, 1304, 1181, 1093, 958, 902, 757, 602, 477, 461 cm^{-1} ; UV (λ_{max}) nm: 232.7,

277.1, 303.2 nm; $^1\text{H-NMR}$ (CDCl_3 , 500 MHz) δ : 6.11 (s, 1H), 7.22-7.34 (m, 5H), 7.36-7.44 (m, 4H), 7.60-7.66 (m, 2H), 8.00 (d, 1H, $J= 7.5$ Hz), 8.07 (d, 1H, $J= 7.5$ Hz), 11.29 (s, 1H, exchangeable with D_2O), 11.52 (s, 1H, exchangeable with D_2O); $^{13}\text{C-NMR}$ (DMSO, 125 MHz) δ : 36.2, 116.6, 124.4, 124.9, 126.5, 126.9, 128.7, 132.8, 132.9, 135.2, 141.2, 152.5, 163.1, 164.7; MS (ESI): m/z 413 $[\text{M}+\text{H}]^+$.

4.3. Density functional theory calculations

The Gaussian 09 program package was used to perform all calculations [44]. The equilibrium geometries of all compounds were calculated using the B3LYP functional in conjunction with the 6-311+G(d,p) basis set [45]. Simulations of UV-Vis spectra were performed using TD-DFT and structures optimized in methanol, since experimental spectra were acquired using this solvent.

4.4. Biological experiments

4.4.1. *In vitro* assays

The compounds were dissolved in DMSO. All tests were undertaken on three replicates, the results were averaged and standard deviation was considered to be less than 10%.

1) Antilipid peroxidation. Production of conjugated diene hydroperoxide by oxidation of linoleic acid in an aqueous dispersion is monitored at 234 nm. AAPH is used as a free radical initiator. Linoleic acid sodium salt solution (10 ml of 16 mM) was added to the UV cuvette containing 0.93 ml of 0.05 M phosphate buffer, pH 7.4 pre-thermostated at 37°C . The oxidation reaction was initiated at 37°C under air by the addition of 50 μl of 40 mM AAPH solution. Oxidation was carried out in the presence of aliquots (10 μl) in the assay without antioxidant. Lipid oxidation was measured in the presence of the same level of DMSO. The rate of oxidation at 37°C was monitored by recording the increase in absorption at 234 nm caused by conjugated diene hydroperoxides and compared with the appropriate standard Trolox [40 a,b].

2) Lipoxygenase inhibition. The tested compounds were incubated at room temperature with sodium linoleate (100 μl) and 200 μl of enzyme LOX type Ib solution ($1/9 \times 10^{-4}$ w/v in saline) and buffer tris pH 9. The conversion of sodium linoleate to 13- hydroperoxylinoleic acid at 234 nm was recorded and compared with the appropriate standard inhibitor NDGA [40 a,b]. Several concentrations were used in order to determine IC_{50} values of the more potent compounds.

4.3. Molecular modeling experiments

4.3.1. Soybean lipoxygenase crystal structure preparation

To the best of our knowledge, there are no crystal structures containing co-crystallized structures of compounds investigated in this study with soybean lipoxygenase. Therefore, molecular docking was performed on soybean lipoxygenase-Ib (PDB ID: **5T5V**). Initially, protein was

prepared for molecular modelling after being loaded into the UCSF Chimera v1.10.1 software [46] for Linux 64 bit architecture and visually inspected. Protein was then energy minimized as follows: through the leap module of the Amber suite [47] they were solvated with water molecules (TIP3 model, SOLVATEOCT Leap command) in a box extending 10 Å in all directions, neutralized with either Na⁺ or Cl⁻ ions, and refined by a single point minimization using the Sander module with maximum 1000 steps of the steepest-descent energy minimization followed by maximum 4000 steps of conjugate-gradient energy minimization, with a non-bonded cut off of 5 Å.

4.3.2. Generation of dicoumarol derivatives structures

All of the dicoumarol derivatives structures were modeled by applying the Chemaxon's msketch module [48] by means of molecular mechanics' optimization upon which the hydrogen atoms, appropriate for pH 7.4, were assigned.

4.3.3. Molecular docking protocol

The active site definition was performed upon the **5T5V** crystal had been aligned to soybean lipoxygenase-3 co-crystallized with 13(s)-hydroperoxy-9(Z),11(E)-octadecadienoic acid (PDB ID: **1IK3**) [49], by means of UCSF Chimera MatchMaker module. The protein part of **1IK3** crystal was prepared similarly to the **5T5V** one. Thus, an **1IK3** inhibitor was extracted from the complex after which either protein or ligand were improved by assigning the hydrogen atoms at pH of 7.4 and Amber parameters [47] using Antechamber semi-empirical QM method. Upon the thorough examination, the A chain of each complex was retained for further manipulation and aligned to obtain common relative coordinates.

The prepared structures of **5T5V** and **1IK3** were imported into AutoDockTools graphical user interface. Nonpolar hydrogen atoms were removed while Gasteiger charges and solvent parameters were added. All of the tested compounds were used as ligands for docking. The rigid root and rotatable bonds were defined using AutoDockTools. The docking on **5T5V** was performed with AutoDock 4.2 [50] by applying the cuboid docking grid coordinates provided from **1IK3** complex as follows: the xyz coordinates (in Ångströms) for the computation were Xmin/Xmax = 8.328/31.096, Ymin/Ymax = -15.291/15.029, Zmin/Zmax = 3.579/31.555; the coordinates setup was performed in a manner to embrace the minimized inhibitor spanning 10 Å in all three dimensions. The Lamarckian Genetic Algorithm was used to generate orientations or conformations of ligands within the binding site. The procedure of the global optimization started with a sample of 200 randomly positioned individuals, a maximum of 1.0×10^6 energy evaluations and a maximum of 27 000 generations. A total of 100 runs were performed with RMS Cluster Tolerance of 0.5 Å.

4.3.4. Molecular dynamics protocol

The merged ligand-Lox-Ib complexes were used to perform explicit solvent molecular dynamics simulations. The parallelized Desmond Molecular Dynamics System and associated analysis tools, available within the Schrödinger suite 2009 [51], were used for this purpose. The models were prepared using the 'system builder' utility. The OPLS_2005 force field parameters were assigned for all the simulation systems. Each inhibitors-enzyme complex was placed in the centre of a orthorhombic box ensuring 10 Å solvent buffers between the solute and the boundary of simulation box in each direction. The TIP3 model was used to describe the water molecules. More, Na⁺ and Cl⁻ ions were added at physiological concentration of 0.15 M to neutralize. The model systems were relaxed using to 0.5 Å using the minimization protocol and subjected to a production phase, using the NPT ensemble and periodic boundary conditions for a period of 1.2 ns. The pressure control was used to maintain the pressure of the cell at 1.013 bar using the isotropic coupling method. The Nose-Hoover thermostat method was used to control the temperature at 310.15 K. Heavy atom-hydrogen covalent bonds were constrained using the SHAKE algorithm which allowed a 2-fs integration step to be used. The integration of the equation of motion as implemented according to the RESPA multiple time step scheme was used in the simulations. Long-range electrostatic forces were computed using the smooth Particle-Mesh Ewald (PME) method. The cutoff distance for calculating short-range electrostatics and Lennard-Jones interaction was set to 9.0 Å. The trajectories and the energies were recorded at every 4.8 ps, respectively. The simulation quality analysis tool was used to analyze the trajectories obtaining RMSD and RMSF values, hydrogen bond distances, angles, and van der Waals interactions over the simulation trajectories.

Acknowledgments

This work was supported by the Ministry of Education, Science and Technological Development of the Republic of Serbia (Projects No. 172016 and III43004).

References

[1] (a) D.H. Murray, J. Mendez, S.A. Brown, *The Natural Coumarins: Occurrence, Chemistry and Biochemistry*, J. Wiley & Sons, N. York, 1982, pp. 1; (b) R. O'Kennedy, R.D. Thornes, "Coumarins: Biology, Applications and Mode of Action", J. Wiley & Sons, Chichester, 1997, pp. 1; (c) K.C. Fylaktakidou, D.J. Hadjipavlou-Litina, K.E. Litinas, D.N. Nicolaidis, *Natural and synthetic coumarin derivatives with anti-Inflammatory/antioxidant activities*, *Curr. Pharm. Design* 10 (2004) 3813–3833; (d) F. Borges, F. Roleira, N. Milhazes, L. Santana, E. Uriarte, *Simple coumarins and analogues in medicinal chemistry: occurrence, synthesis and biological activity*, *Curr. Med. Chem.* 12 (2005) 887–916; (e) X.-S. Zhang, Z.-W Li, Z.-J. Shi, *Palladium-catalyzed base-accelerated direct C–H bond alkenylation of phenols to synthesize coumarin derivatives*, *Org. Chem. Front.* 1 (2014) 44–49.

[2] (a) A. Lacy, R. O'Kennedy, *Studies on coumarins and coumarin-related compounds to determine their therapeutic role in the treatment of cancer*, *Curr. Pharm. Des.* 10 (2004) 3797–

3811; (b) T.V. Orlovskaya, I.L. Luneva, V.A. Chelombit'ko, Chemical composition of *Cynara scolymus* leaves, *Chem. Nat. Compd.* 43 (2007) 239–240.

[3] (a) D. Wardrop, D. Keeling, The story of the discovery of heparin and warfarin, *Br. J. Haematol.* 141 (2008) 757–763; (b) A.M. Holbrook, J.A. Pereira, R. Labiris, H. McDonald, J.D. Douketis, M. Crowther, P.S. Wells, Systematic overview of warfarin and its drug and food interactions, *Arch. Intern. Med.* 165 (2005) 1095–1106; (c) O.M. Abdelhafez, K.M. Amin, R.Z. Batran, T.J. Maher, S.A. Nada, S. Sethumadhavan, Synthesis, Anticoagulant and PIVKA-II induced by new 4-hydroxycoumarin derivatives, *Bioorg. Med. Chem.* 18 (2010) 3371–3378.

[4] P.Y. Lin, K.-S. Yeh, C.-L. Su, S.-Y. Sheu, T. Chen, K.-L. Ou, M.-H. Lin, L.-W. Lee, Synthesis and antibacterial activities of novel 4-hydroxy-7-hydroxy- and 3-carboxycoumarin derivatives, *Molecules* 17 (2012) 10846-10863.

[5] Z.H. Chohan, A.U. Shaikh, A. Rauf, C.T. Supuran, Antibacterial, antifungal and cytotoxic properties of novel N-substituted sulfonamides from 4-hydroxycoumarin, *J. Enzyme Inhib. Med. Chem.* 21 (2006) 741–748.

[6] (a) B.S. Kirkiacharian, E. Clercq, R. Kurkjian, C. Pannecouque, New synthesis and anti-HIV and antiviral properties of 3-arylsulfonyl derivatives of 4-hydroxycoumarin and 4-hydroxyquinolone, *Pharm. Chem. J.* 42 (2008) 265–270; (b) D. Završnik, S. Muratović, D. Makuc, J. Plavec, M. Cetina, A. Nagl, E. De Clercq, J. Balzarini, M. Mintas, Benzylidene-bis-(4-hydroxycoumarin) and benzopyranocoumarin derivatives: synthesis, $^1\text{H}/^{13}\text{C}$ -NMR conformational and x-ray crystal structure studies and in vitro antiviral activity evaluations, *Molecules* 16 (2011) 6023-6040.

[7] A.K. Arya, K. Rana, M. Kumar, A facile synthesis and anticancer activity evaluation of spiro analogs of benzothiazolylchromeno/ pyrano derivatives, *Lett. Drug Des. Discov.* 11 (2014) 594–600.

[8] F.S. Senol, G. Yilmaz, B. Sener, M. Koyuncu, I. Orhan, Preliminary screening of acetylcholinesterase inhibitory and antioxidant activities of Anatolian Heptaptera species, *Pharm. Biol.* 48 (2010) 337–341.

[9] V.D. Kancheva, P.V. Boranova, J.T. Nechev, I.I. Manolov, Structure-activity relationships of new 4-hydroxy bis-coumarins as radical scavengers and chain-breaking antioxidants, *Biochimie*, 92 (2010) 1138–1146.

[10] R. Ahmad, M. Asad, Z.N. Siddiqui, A. Kumar, Screening of synthetic new heterocyclic derivatives of 3-formyl-4-hydroxycoumarin for anti-inflammatory activity in albino rats, *JPRHC* 1 (2009) 46–62.

- [11] M. Ufer, Comparative pharmacokinetics of vitamin K antagonists: warfarin, phenprocoumon and acenocoumarol, *Clin. Pharmacokinet.* 44 (2005) 1227–1246.
- [12] M. Beinema, J.R. Brouwers, T. Schalekamp, B. Wilffert, Pharmacogenetic differences between warfarin, acenocoumarol and phenprocoumon, *Thromb. Haemost.* 100 (2008) 1052–1057.
- [13] N. Kresge, R.D. Simoni, R.L. Hill, Hemorrhagic sweet clover disease, dicoumarol, and warfarin: The work of Karl Paul Link, *J. Biol. Chem.* 280 (2005) e5–e6.
- [14] R.B. Arora, N.R. Krishnaswamy, T.R. Seshadri, S.D.S. Seth, B.R. Sharma, Structure and anticoagulant activity of bridge-substituted dicoumarols, *J. Med. Chem.* 10 (1967) 121–124.
- [15] I. Kostova, Synthetic and natural coumarins as cytotoxic agents, *Curr. Med. Chem.-Anti-Cancer Agents*, 5 (2005) 29–46.
- [16] A. Mazumder, S. Wang, N. Neamati, M. Nicklaus, S. Sunder, J. Chen, G.W.A. Milne, W.G. Rice, Jr.T.R. Burke, Y. Pommier, Antiretroviral agents as inhibitors of both human immunodeficiency virus type 1 integrase and protease, *J. Med. Chem.* 39 (1996) 2472–2481.
- [17] K.M. Khan, S. Iqbal, M.A. Lodhi, G.M. Maharvi, Z. Ullah, M.I. Choudhary, A. Rahmana, S. Perveen, Biscoumarin: new class of urease inhibitors; economical synthesis and activity, *Bioorg. Med. Chem.* 12 (2004) 1963–1968.
- [18] A. Kumar, M.K. Gupta, M. Kumar, Synthesis and biological evaluation of N-aryl-1, 4-dihydropyridines as novel antidiabetic and antioxidant agents, *Tetrahedron Lett.* 52 (2011) 4521–4525.
- [19] M. Kidwai, V. Bansal, P. Mothra, S. Saxena, R.K. Somvanshi, S. Dey, T.P. Singh, Molecular Iodine: A Versatile Catalyst for the Synthesis of Bis(4-Hydroxycoumarin) Methanes in Water, *J. Mol. Catal. A* 268 (2007) 76–81.
- [20] (a) K.P. Boroujeni, P. Ghasemi, Synthesis and application of a novel strong and stable supported ionic liquid catalyst with both Lewis and Brønsted acid sites, *Catal. Commun.* 37 (2013) 50–54; (b) Z.N. Siddiqui, Sulfamic acid catalysed synthesis of pyranocoumarins in aqueous media, *Tetrahedron Lett.* 55 (2014) 163–168.
- [21] W. Li, Y. Wang, Z.Z. Wang, L.Y. Dai, Y.Y. Wang, Novel SO₃H-functionalized ionic liquids based on benzimidazolium cation: Efficient and recyclable catalysts for one-pot synthesis of biscoumarin derivatives, *Catal. Lett.* 141 (2011) 1651–1658.
- [22] Z.N. Siddiqui, F. Farooq, Zn(Proline)₂: A novel catalyst for the synthesis of dicoumarols, *Catal. Sci. Technol.* 1 (2011) 810–816.

- [23] P. Singh, P. Kumar, A. Katyal, R. Kalra, S.K. Dass, S. Prakash, R. Chandra, Phosphotungstic acid: an efficient catalyst for the aqueous phase synthesis of bis-(4-hydroxycoumarin-3-yl)methanes, *Catal. Lett.* 134 (2010) 303–308.
- [24] H. Mehrabi, H. Abusaidi, Synthesis of biscoumarin and 3,4-dihydropyrano[c]chromene derivatives catalysed by sodium dodecyl sulfate (SDS) in neat water, *J. Iran. Chem. Soc.* (2010) 890–894.
- [25] B. Karmakar, A. Nayak, J. Banerji, Sulfated titania catalyzed water mediated efficient synthesis of dicoumarols - a green approach, *Tetrahedron Lett.* 53 (2012) 4343–4346.
- [26] (a) R. Karimian, F. Piri, A.A. Safari, S.J. Davarpanah, One-pot and chemoselective synthesis of bis(4-hydroxycoumarin) derivatives catalyzed by nano silica chloride, *J. Nanostruct. Chem.* 3 (2013) 52–57; (b) . G. M Ziarani, A. Badiei, M. Azizia, N. Lashgari, Efficient one-pot synthesis of bis(4-hydroxycoumarin)methanes in the presence of sulfonic acid functionalized nanoporous silica (SBA-Pr-SO₃H), *J. Chin. Chem. Soc.* 60 (2013) 499–502.
- [27] R. Rezaei, F. Moezzi, M.M. Doroodmand, *Chin. Chem. Lett.* 184 (2014) 183–186.
- [28] Z. Karimi-Jaberi, M.R. Nazarifar, Efficient catalysts for the rapid synthesis of benzylidene bis(4-hydroxycoumarin) derivatives. in aqueous media, *Eur. Chem. Bull.* 3 (2014) 512–514.
- [29] S. Khodabakhshi, B. Karami, K. Eskandari, S. J. Hoseini, H. Nasrabadi, *Arab. J. Chem.* 2014, in press, <https://doi.org/10.1016/j.arabjc.2014.05.030>.
- [30] H. Zahao, N. Neamati, H. Hong, A. Mazumder, S. Wang, S. Sunder, G.W. A. Milne, Y. Pommier, T.R. Ir. Burke, Coumarin-based inhibitor of HIV integrase. *J. Med. Chem.* 40 (1997) 242–249.
- [31] M.N. Elinson, A.N. Vereshchagin, O.O. Sokolova, Fast highly efficient ‘on-solvent’ non-catalytic cascade transformation of benzaldehydes and 4-hydroxycoumarin into bis(4-hydroxycoumarinyl)arylmethanes, *Arkivoc*, 3 (2017) 121–129.
- [32] A. Das Gupta, S. Samanta, R. Mondal, A.K. Mallik, A Convenient, Eco-friendly, and efficient method for synthesis of 3,3'-arylmethylene-bis-4-hydroxycoumarins “On-water”, *Bull. Korean Chem. Soc.* 33 (2012) 4239–4242.
- [33] S. Qadir, A.A. Dar, K.Z. Khan, Synthesis of bis- coumarins from 4-hydroxycoumarin and aromatic aldehydes - A comparative assessment of percentage yield under thermal and microwave-assisted conditions, *Synthetic Commun.* 38 (2008) 3490–3499.

- [34] A. Shamsaddini, E. Sheikhhosseini, Synthesis of 3,3-arylidene bis(4-hydroxycoumarin) catalyzed by p-dodecylbenzenesulfonic acid (DBSA) in aqueous media and microwave irradiation, *Int. J. Org. Chem.* 4 (2014) 135–141.
- [35] A.D. Gupta, S. Samanta, R. Mondal, A.K. Mallik, An efficient and eco-friendly synthesis of 2-arylbenzimidazoles using silica gel as catalyst, *Chem. Sci Trans.*, 2 (2013) 524–528.
- [36] (a) A. de la Hoz, A. Diaz-Ortiz, P. Prieto, “Microwave-assisted Green Organic Synthesis, in Alternative Energy Sources for Green Chemistry”, ed. G. Stefanidis, A. Stankiewicz, RSC Green Chemistry No. 47, Cambridge, UK, 2016, ch. 1, pp 1–33; (b) N.E. Leadbeater, “Organic Synthesis Using Microwave Heating, in Comprehensive Organic Synthesis”: 2nd edn., ed. P. Knochel, G. Molander, Elsevier Ltd., Oxford, 2014, ch. 10, vol. 9, pp. 234–286; (c) C. O. Kappe, C. O.; Stadler, A. “Microwaves in Organic and Medicinal Chemistry”, Wiley, Weinheim, 2nd edn, 2012.
- [37] I. Ahmad, S.A. Nawaz, N. Afza, A. Malik, I. Fatima, S.B. Khan, M. Ahmad, M.I. Choudhary, Isolation of Onosmins A and B, Lipoxygenase Inhibitors from *Onosma hispidum*, *Chem. Pharm. Bull.* 53 (2005) 907–910.
- [38] (a) D. Steinhilber, 5-Lipoxygenase: a target for antiinflammatory drugs revisited, *Curr. Med. Chem.* 6 (1999) 71–85; (b) Y.X. Ding, G.W. Tong, E.T. Adrian, Cyclooxygenases and lipoxygenases as potential targets for treatment of pancreatic cancer, *Pancreatology* 1 (2001) 291–296; (c) D. Wang, R.N. DuBois, Eicosanoids and cancer. *Nat. Rev. Cancer* 10 (2010) 181–193.
- [39] (a) P. Srivastava, V.K. Vyas, B. Variya, P. Patel, G. Qureshi, M. Ghate, Synthesis, anti-inflammatory, analgesic, 5-lipoxygenase (5-LOX) inhibition activities, and molecular docking study of 7-substituted coumarin derivatives, *Bioorg. Chem.* 67 (2016) 130–138; (b) R. Torres, C. Mascayano, C. Núñez, B. Modak, F. Faini, Coumarins of *haplopappus multifolius* and derivative as inhibitors of LOX: evaluation *in-vitro* and docking studies, *J. Chil. Chem. Soc.*, 58 (2013) 2027–2030; (c) N.P. Reddy, T.C. Reddy, P. Aparoy, C. Achari, P.R. Sridhar, P. Reddanna, Structure based drug design, synthesis and evaluation of 4-(benzyloxy)-1-phenylbut-2-yn-1-ol derivatives as 5-lipoxygenase inhibitors, *Eur. J. Med. Chem.* 47 (2012) 351.
- [40] (a) G.A. Veldink, J.F.G. Vliegenter, A.A. Finazzi, *Lipids* 30 (1995) 51–54; (b) S.G. Rival, C.G. Boeriu, H.J. Wichers, *J. Agric. Food Chem.* 49 (2001) 295–302; (c) M. Maccarrone, A. Baroni, A. Finazzi-Agro, *Arch. Biochem. Biophys.* 356 (1998) 35–40; (d) T.J. Ha, I. Kubo, *J. Agric. Food Chem.* 55 (2007) 446–451.
- [41] (a) T. Balalas, A. Abdul-Sada, D.J. Hadjipavlou-Litina, K.E. Litinas, Synthesis, Pd-Catalyzed efficient synthesis of azacoumestans *via* intramolecular cross coupling of 4-(arylamino)coumarins in the presence of copper acetate under microwaves, 49 (2017) 2575–

2583; (b) T.S. Symeonidis, D.J. Hadjipavlou-Litina, K.E. Litinas, Synthesis through three-component reactions catalyzed by FeCl_3 of fused pyridocoumarins as inhibitors of lipid peroxidation, *J. Heterocyclic Chem.* 51 (2014) 642–647; (c) T.S. Symeonidis, K.E. Litinas, Synthesis of methyl substituted [5,6]- and [7,8]-fused pyridocoumarins *via* the iodine-catalyzed reaction of aminocoumarins with n-butyl vinyl ether, *Tetrahedron Lett.* 54 (2013) 6517–6519.

[42] J.K. Verma, K. Raghuvanshi, R.K. Verma, P. Dwivedi, M.A. Singh, An efficient one-pot solvent-free synthesis and photophysical properties of 9-aryl/alkyl-octahydroxanthene-1,8-diones, *Tetrahedron*, 2011, 67, 3698-3704.

[43] A.R. Offenbacher, S. Hu, E.M. Poss, C.A.M. Carr, A.D. Scouras, D.M. Prigozhin, A.T. Iavarone, A. Palla, T. Alber, J.S. Fraser, J.P. Klinman, Hydrogen–deuterium exchange of lipoxigenase uncovers a relationship between distal, solvent exposed protein motions and the thermal activation barrier for catalytic proton-coupled electron tunneling, *ACS Cent. Sci.* 3 (2017) 570–579.

[44] M. J. Frisch, W. G. Trucks, B. H. Schlegel, E. G. Scuseria, A. M. Robb, R. J. Cheeseman, G. Scalmani, V. Barone, B. Mennucci, A. G. Petersson, H. Nakatsuji, M. Caricato, X. Li, P. H. Hratchian, F. A. Izmaylov, J. Bloino, G. Zheng, L. J. Sonnenberg, M. Hada, M. Ehara, K. Toyota, R. Fukuda, J. Hasegawa, M. Ishida, T. Nakajima, Y. Honda, O. Kitao, H. Nakai, T. Vreven, A. J. Montgomery Jr., E. J. Peralta, F. Ogliaro, M. Bearpark, J. J. Heyd, E. Brothers, N. K. Kudin, N. V. Staroverov, R. Kobayashi, J. Normand, K. Raghavachari, A. Rendell, C. J. Burant, S. S. Iyengar, J. Tomasi, M. Cossi, N. Rega, J. M. Millam, M. Klene, J. E. Knox, J. B. Cross, V. Bakken, C. Adamo, J. Jaramillo, R. Gomperts, E. R. Stratmann, O. Yazyev, J. A. Austin, R. Cammi, C. Pomelli, W. J. Ochterski, L. R. Martin, K. Morokuma, G. V. Zakrzewski, A. G. Voth, P. Salvador, J. J. Dannenberg, S. Dapprich, D. A. Daniels, O. Farkas, B. J. Foresman, V. J. Ortiz, J. Cioslowski, J. D. Fox, Gaussian 09, Rev C Gaussian Inc., Wallingford, 2009.

[45] (a) C. Lee, W. Yang and R. G. Parr, Development of the Colle-Salvetti correlation-energy formula into a functional of the electron density, *Phys. Rev. B* 37 (1988) 785; (b) A. D. Becke, Density-functional thermochemistry. III. The role of exact exchange, *J. Chem. Phys.* 98 (1993) 5648.

[46] E.F. Pettersen, T.D. Goddard, C.C. Huang, G.S. Couch, D.M. Greenblatt, E.C. Meng, T.E. Ferrin, UCSF Chimera - A visualization system for exploratory research and analysis. *J. Comput. Chem.* 25 (2004) 1605–1612.

[47] D.A. Case, T.A. Darden, T.E.III Cheatham, C.L. Simmerling, J. Wang, R.E. Duke, R. Luo, R.C. Walker, W. Zhang, K.M. Merz, B. Roberts, S. Hayik, A. Roitberg, G. Seabra, J. Swails, A. W. Götz, I. Kolossváry, K.F. Wong, F. Paesani, J. Vanicek, R.M. Wolf, J. Liu, X. Wu, S.R. Brozell, T. Steinbrecher, H. Gohlke, Q. Cai, X. Ye, J. Wang, M.-J. Hsieh, G. Cui, D.R. Roe,

D.H. Mathews, M.G. Seetin, R. Salomon-Ferrer, C. Sagui, V. Babin, T. Luchko, S. Gusarov, A. Kovalenko, P.A. Kollman, AMBER 12, University of California, San Francisco. **2012**.

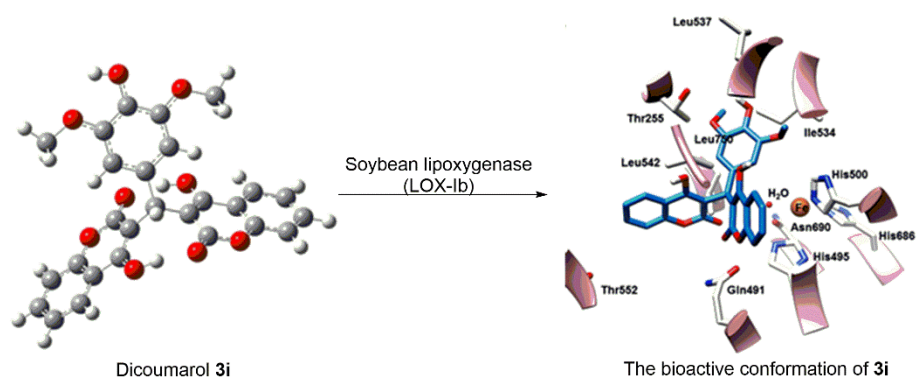
[48] Marvin Beans 15.4.27.0, 2015, Chem Axon (<http://www.chemaxon.com>), Date of Access January 2015.

[49] E. Skrzypczak-Jankun, R.A. Bross, R.T. Carroll, W.R. Dunham, M.O. Funk, Jr. Three-Dimensional structure of a purple lipoxygenase *J. Am. Chem. Soc.*, 123 (2001) 10814–10820.

[50] G.M. Morris, R. Huey, W. Lindstrom, M.F. Sanner, R.K. Belew, D.S. Goodsell, A.J. Olson, AutoDock4 and AutoDockTools4: automated docking with selective receptor flexibility. *J. Comput. Chem.* 16 (2009) 2785–2791.

[51] F. Mohamadi, N.G.J. Richards, W.C. Guida, R. Liskamp, M. Lipton, C. Caufield, et al., Macromodel-an integrated software system for modeling organic and bioorganic molecules using molecular mechanics, *J. Comput. Chem.* 11 (1990) 440-467.

Graphical abstract



ACCEPTED MANUSCRIPT

Highlights

- Dicoumarol derivatives were synthesized in green InCl_3 catalyzed reaction.
- Structures of all obtained products were elucidated by spectroscopic techniques.
- Dicoumarols were subjected to evaluation of their *in vitro* lipid peroxidation and soybean lipoxygenase inhibition activities.
- The bioactive conformations of the best LOX inhibitors were obtained by means of molecular docking and molecular dynamics.